The Mechanism of Protraction of Insulin Detemir, a Long-acting, Acylated Analog of Human Insulin

Svend Havelund,[1,2] Anne Plum,[1] Ulla Ribel,[1] Ib Jonassen,[1] Aage Vølund,[1] Jan Markussen,[1] and Peter Kurtzhals[1]

Received March 3, 2004; accepted April 9, 2004

Purpose. Insulin detemir has been found in clinical trials to be absorbed with very low variability. A series of experiments were performed to elucidate the underlying mechanisms.

Methods. The disappearance from an injected subcutaneous depot and elimination studies in plasma were carried out in pigs. Size-exclusion chromatography was used to assess the self-association and albumin binding states of insulin detemir and analogs.

Results. Disappearance $T_{50\%}$ from the injection depot was 10.2 ± 1.2 h for insulin detemir and 2.0 ± 0.1 h for a monomeric acylated insulin analog. Self-association of acylated insulin analogs with same albumin affinity in saline correlated with disappearance rate and addition of albumin to saline showed a combination of insulin detemir self association and albumin binding. Intravenous kinetic studies showed that the clearance and volume of distribution decreased with increasing albumin binding affinity of different acylated insulin analogs.

Conclusions. The protracted action of detemir is primarily achieved through slow absorption into blood. Dihexamerization and albumin binding of hexameric and dimeric detemir prolongs residence time at the injection depot. Some further retention of detemir occurs in the circulation where albumin binding causes buffering of insulin concentration. Insulin detemir provides a novel principle of protraction, enabling increased predictability of basal insulin.

KEY WORDS: albumin binding; insulin detemir; insulin pharmacokinetics; insulin self-association; protracted action.

INTRODUCTION

The peptide hormone, insulin, is produced and stored in pancreatic beta-cells. An adaptation of beta-cell insulin production is the assembly of insulin molecules at high concentration in the presence of zinc ions into hexamers (1). This process provides efficient spatial storage within beta-cell vesicles, but dilution upon exocytosis ensures immediate dissociation into biologically active monomers. When human insulin is injected into the subcutis in the form of a high-concentration pharmaceutical formulation it is self-associated, and here dissociation into monomers is relatively slow (2,3). Hexamers and dimers of insulin are slower to penetrate the capillary wall than monomers (4), and the rate of entry into the systemic circulation is dependent on local environmental factors. The pharmacokinetic plasma profile following a standardized injection of human insulin reflects the rate of absorption and shows considerable variation both between and within individuals (5,6).

The advent of recombinant DNA technology in the 1980s enabled the molecular structure of insulin to be manipulated, and attempts were made to modify regions believed to function as self-association binding surfaces not involved in ligand-receptor interaction (4,7). By the late 1990s, the clinically available rapid-, short-acting analogs, insulin aspart and insulin lispro, had been developed. These agents, with increased dissociation rate-constants, are relatively quickly absorbed from the subcutis and, when administered immediately before meals, are able to mimic the prandial peaks of insulin secretion seen in normal physiology (8–10).

More recently, attempts have been made to develop insulin analogs with protracted absorption from the subcutis, to better imitate the basal insulin profile. Previously, protamine (neutral protamine Hagedorn [NPH]) or an excess of zinc (Lente, Ultralente insulin) had been added to form suspension preparations of insulin with delayed dissolution and absorption. However, this first generation of basal insulin formulations poorly mimics the low, constant overnight plasma insulin profile seen in normal physiology (11–14). NPH insulin, for example, is characterized by a pharmacokinetic profile that peaks 4–6 h after injection, followed by a steady decline (15). Its absorption rate varies unpredictably over time, creating poorly reproducible kinetic profiles (11). Inter- and intrasubject variability is exacerbated further by inconsistencies in resuspension prior to injection (12,14). Such variations increase the risk of hypoglycemic events, particularly nocturnal ones following evening administration, and limit glycemic control.

Two strategies to protract absorption by bioengineering the insulin molecule have been tested clinically. The first principle was to shift the isoelectric point of the molecule toward neutrality to provide reduced solubility at physiological pH values. Clinical development for the first analogs based on this principle was discontinued because of low bioavailability and variability of action (16,17). The same principle was later used for insulin glargine (Gly^{A21} Arg^{B31} Arg^{B32} human insulin), in which two arginine residues added to the C-terminus of the B-chain, shift the isoelectric point from pH 5.4 to 6.7 (12,15,18–20). Glargine is injected as an acid solution (pH 4.0), and forms a slowly absorbed precipitate in the neutral environment of the subcutis. This property means that it cannot be mixed with neutral formulations of other insulins.

A more recent strategy has been to acylate fatty acid species to the insulin molecule to allow insulin-albumin binding in an attempt to protract the time-action profile while retaining the practical advantages of a neutral liquid preparation (21,22). The time for 50% disappearance after subcutaneous injection in pigs was longer than that of NPH insulin and with less interpig variation (22). The first clinically available acylated analog is insulin detemir [Lys^{B29}(*N*-tetradecanoyl)des(B30)human insulin], in which the amino acid threonine at B30 is removed, and a 14-carbon, myristoyl fatty acid is acylated to lysine at B29. A lower pharmacokinetic and pharmacodynamic variability of insulin detemir relative to NPH insulin was reported (14,37).

At therapeutic doses, detemir occupies only a tiny frac-

[1] Research and Development, Novo Nordisk A/S, Bagsvaerd, Denmark.

[2] To whom correspondence should be addressed. (e-mail: svh@novonordisk.com)

ABBREVIATIONS: HSA, human serum albumin; PSA, porcine serum albumin; NPH, neutral protamine Hagedorn insulin; SEC, size-exclusion chromatography; APL, a programming language.

0724-8741/04/0800-1498/0 © 2004 Plenum Publishing Corporation

tion of albumin binding sites and has not shown any clinically relevant interactions with other albumin-bound drugs (23). Kinetic and euglycemic clamp comparisons with NPH insulin have confirmed that insulin detemir is more protracted and has flatter pharmacokinetic and time-action profiles in man (24,25), but the exact mechanism underlying this has not been fully elucidated. Although delayed trans-endothelial transport from blood into interstitium has been clearly demonstrated (26–28), acylation may also enable albumin binding to occur at the injection site depot and in the distal interstitial fluid, and these too could protract the pharmacodynamic profile of detemir. It is also possible that interactions could occur between detemir's myristoyl fatty acid side chains to form hexamer aggregates at the injection depot, and the use of zinc, phenol, and other stabilizers in the pharmaceutical formulation might further modify the kinetics of absorption. A number of physicochemical and pharmacokinetic experiments were therefore conducted in an attempt to further elucidate the mechanism of protraction of insulin detemir following subcutaneous injection.

MATERIALS AND METHODS

Research Design

The self-association and albumin binding states of insulin detemir in the injection depot, at the depot-interstitial fluid junction and in plasma were modeled using size-exclusion chromatography. Subcutaneous disappearance of insulin detemir was assessed in a pig model and compared to analogs with different propensity for self-association, but with similar albumin binding affinities. The plasma insulin profile of insulin detemir was measured following intravenous bolus administration in pigs and compared to analogs with different albumin binding affinities. Data generated from these different methods were to be integrated with prior knowledge to construct a hypothesis describing the protracted kinetic profile of insulin detemir.

Insulin Preparations

Insulin analogs were constructed by oligonucleotide-directed mutagenesis, fermented in yeast, purified, and acylated using previously described methodology (4,16,17,29). Corresponding ^{125}I-labeled tracers (labeled at Tyr^{A14}) were prepared as described by Drejer *et al.* (30). Solutions of pH 7.5 containing 600 μM of insulin analog, 2 Zn^{2+}/hexamer, 1.6% glycerol, 16 mM phenol, 16 mM *m*-cresol, and 7 mM sodium phosphate were used in testing pharmacokinetic properties. The mono^{125}I-Tyr^{A14}-insulin-tracers and $^{65}Zn^{2+}$ were added to 37 kBq/ml before the preservatives. Co(III)-insulin was prepared according to previously described methodology (31). The experimental insulin analogs are here referred to by designated Novo Nordisk code numbers.

Albumin Binding

Binding constants were determined using fatty acid-free human (HSA) and porcine serum albumin (PSA) immobilized on divinylsulfone activated Sepharose 6B. Constants were determined as bound and free mono^{125}I-Tyr^{A14}-insulin-analog-tracer as a function of immobilized albumin concentration. The association constants were expressed relative to insulin detemir ($K_a = 1.0 \pm 0.3 \times 10^5$ M^{-1} at 37°C for HSA) (21,22).

Size-Exclusion Chromatography

Size-exclusion chromatography (SEC) was used to assess the self-association and albumin binding states of insulin detemir at various conditions designed to model events at the site of subcutaneous injection. The factor of self-association was investigated by manufacturing a series of insulin analogs with about the same albumin binding, but decreasing propensity to self-association. The analogs were made by acylation with a C14 fatty acid moiety of human insulin analogs with decreasing self-association propencity: insulin detemir (Lys^{B29}(*N*-tetradecanoyl) des(B30) human insulin), O368 (Gly^{B1} Lys^{B29}(*N*-tetradecanoyl) des(B30) human insulin), O381 (Asp^{B28} Lys^{B29}(*N*-tetradecanoyl) des(B30) human insulin), and O437 (His^{A8} Glu^{B1} Glu^{B10} Glu^{B16} Glu^{B27} Lys^{B29}(*N*-tetradecanoyl) des(B30) human insulin) (4,22,34), and the relative albumin binding affinities were found to 1.0, 1.0, 1.3, and 0.9, respectively).

The pharmaceutical formulation of insulin detemir includes zinc, sodium chloride, phosphate buffer, preservatives, and a polyol isotonic. It is assumed that, following injection, small, fast-diffusing free or loosely bound species are depleted from the solvent through blood capillaries while sodium chloride enters the depot to equilibrate an isotonic concentration. Therefore, elution profiles of the test analogs were determined with 2 mM phenol and without phenol added to the isotonic saline eluent to simulate the effect of solute exchange.

The albumin binding states of insulin detemir was assessed by including albumin (HSA) in the eluent. To simulate the environment at the mixing zone between the injected depot and the interstitial fluid, albumin was added to the eluent at 150 μM, corresponding to reported level (35). In a series of four experiments, tracers for zinc ($^{65}Zn^{2+}$) or insulin detemir (mono-^{125}I-Tyr^{A14}) were added separately to samples of formulated insulin detemir and eluent. In the latter experiments, insulin detemir was used in nanomolar concentrations to simulate total dissociation.

In SEC, molecules are eluted as a function of their size (Stoke's radius), with larger molecules eluted earlier than smaller substances and linear peptides earlier than globular forms. Insulin detemir and albumin complexes are anticipated to be in globular form (32). The chromatographic system was a Superose 6 HR 10/30 column (Amersham, ambershambiosciences.com) eluted by tris-buffered isotonic saline (NaCl 140 mM, tris/HCl 10 mM, NaN_3 0.01%, pH 7.4, at 37°C), injecting 1% of column volume and using a flow of 90 min per column volume and UV detection at 276 nm or collection of 2 min fractions for gamma counting. The references were a stable monomeric insulin: X2 (Asp^{B9} Glu^{B27} human insulin, zinc free (4)), a stable hexameric insulin: Co(III)-insulin (31), albumin (HSA), and covalent albumin dimer (formed in solution). The references are characterized by the same elution profile irrespective of their concentration and injection volume. In contrast, the elution profile of a normal zinc-phenol/cresol formulation of 600 μM human insulin resembles hexameric Co(III)insulin when injected as 1% of the column volume, but gradually moves to a monomer profile as the injection volume is reduced to 0.06% of the column volume. This reflects dissociation of hexamers into monomers with increasing dilution.

Animal Models

The disappearance and elimination studies were carried out in non-diabetic, conscious, female pigs cross-bred from Danish landrace × Duroc × Yorkshire, weighing 60–100 kg. Before all experiments, the pigs were fasted overnight (18 h).

Disappearance of Subcutaneously Injected Insulin Analogs

It has been previously reported that the absorption course of insulin injected subcutaneously into the neck of pigs is readily comparable with subcutaneous injection in man (36). Therefore, the disappearance rates of a series of labeled insulin detemir formulations and reference injections were measured in this porcine model (Table I). The insulin detemir formulations tested were intended to reflect the gradual change from the pure injected pharmaceutical formulation to its complete mix with the interstitial fluid in the hours following injection. Pigs (n = 5 to 6, for each preparation tested) were injected subcutaneously (dosing volume 100 μl, depth 5–6 mm) on each side of the neck with a radiolabeled insulin preparation enabling each experiment to act as its own reference to normalize data, or over two experimental days by a regular distribution of three samples and the reference. The insulin formulations incorporated γ-emitting tracers as $Tyr^{A14}(^{125}I)$-insulin analog, and the disappearance of radioactivity from the depot was measured continuously as a function of time using a portable Geiger Müller-detector with wireless transmission. The time when 75% or 50% of the radioactivity remains in the depot was calculated for each single disappearance curve and mean values ± SD for each preparation. In the earlier reference experiments cited in Table I a diode-based γ-counter was used. Both of these methods have shown equivalence to a manual method using a NaI(Tl) crystal gamma counter (36).

Plasma Profiles of Acylated Insulin Analogs

Plasma profiles following intravenous bolus administration were determined in groups of 6–7 pigs for $Tyr^{A14}(^{125}I)$-labeled insulin detemir and four analogs O344 (Lys^{B29}(*N*-lithocholoyl-γ-Glu), des(B30) human insulin, O339 (Lys^{B29}(*N*-hexadecanoyl-γ-Glu), des(B30) human insulin), O346 (Lys^{B29}(*N*-ω-carboxy-heptadecanoyl), des(B30) human insulin), O347 (Lys^{B29}(*N*-ω-carboxy-nonadecanoyl), des(B30) human insulin). These analogs were chosen for their range of affinities for porcine serum albumin (PSA) relative to insulin detemir (Table II), and were dosed at 0.36 nmol/kg and 12 kBq/kg. Blood samples were taken at 30 min prior to injection and just after injection every second minute with increasing intervals until 240 min, relative to dose administration. Measurements were made of radioactivity counts (cpm) in trichloroacetic acid (TCA 20%, final concentration 10%) precipitates of 5 ml plasma. Intact insulin analog is present in the precipitate, whereas degradation products show up in the supernatant. In a separate experiment, only unlabeled insulin detemir was injected intravenously and the concentrations in plasma was measured by immunoassay (38) for assessment of the distribution volume.

Previous studies of unlabeled insulin detemir in dogs have shown that a two-compartment model can describe the pharmacokinetics adequately (28). Thus, the elimination of labeled insulin from plasma was described by the model: $C(t) = \alpha_1 \exp(-\beta_1 t) + \alpha_2 \exp(-\beta_2 t)$, where C(t) is the concentration of labeled insulin at time t after i.v. injection. A nonlinear regression computer program written in APL was used for calculation of the values for α_1, α_2, β_1, and β_2 that minimized the weighted sum of squared deviations between the measured concentrations y_i at time t_i and $C(t_i)$ given by the model. The weights were defined as $(1+(y_i/100)^2)^{-1}$ to account for the approximate constant variance at low count rates (<100 CPM) and the approximate constant coefficient of variation

Table I. Disappearance of Labeled, Subcutaneously Injected Insulin Detemir and Insulin Analog Formulations in Pigs

Insulin detemir and analogs with same albumin affinity, but varied self-association	Insulin, formulation and references* (0.6 mM)	$T_{75\%}$ (h, normalized to reference, mean ± SD)	$T_{50\%}$ (h, normalized to reference, mean ± SD)
Detemir in pharmaceutical formulation (hexameric)	Detemir*, 2Zn/hexamer, phenol/cresol, (reference)	4.0 ± 1.0	10.2 ± 1.2
Detemir without preservatives (dihexameric in saline)	Detemir*, 2Zn/hexamer	3.8 ± 0.5	10.5 ± 1.1
Hexameric analog O368 formulated	O368*, 2Zn/hexamer, phenol/cresol		8.8 ± 1.4
Unstable hexameric analog O381 formulated	O381*, 2Zn/hexamer, phenol/cresol		6.9 ± 0.7
Monomeric analog O437 formulated	O437*, 2Zn/hexamer, phenol/cresol	0.9 ± 0.04	2.0 ± 0.1
Detemir and albumin at 0.3 mM (dimeric to hexameric)	Detemir* (0.3 mM), albumin (0.3 mM)	3.0 ± 0.9	7.3 ± 1.6
Detemir below dimeric conc. and 0.3 mM albumin	Detemir* (0.003 mM), albumin (0.3 mM)	1.7 ± 0.3	3.8 ± 0.5
Monomeric analog O437 and albumin at 0.3 mM	O437* (0.3 mM), albumin (0.3 mM)	1.6 ± 0.3	3.7 ± 0.9
†Albumin reference (22)	Albumin* (0.3 mM)	16.5 ± 3.4	43.1 ± 4.5
†Hexameric insulin reference without albumin affinity (31)	Co(III)insulin* (equivalent to 0.6 mM insulin)	1.2 ± 0.3	2.8 ± 0.4
†Monomeric insulin reference without albumin affinity (4)	X2* (0.6 mM)	0.5 ± 0.1	1.0 ± 0.1

* Radioactivity label.
† Reference data from earlier studies.

Table II. Calculated Volume of Distribution, Clearance Rate, and Terminal Long Half-Life of Radiolabeled Acylated Insulin Analogs Following Intravenous Bolus Injection in Pigs

Analog	N	Relative PSA affinity	Volume of distribution (L/kg) mean ± SD	Clearance rate ($ml \cdot min^{-1} \cdot kg^{-1}$) mean ± SD	Terminal half-life (min) mean ± SD
O344	6	0.4	0.052 ± 0.010	1.07 ± 0.20	105 ± 8
Insulin detemir	6	1	0.052 ± 0.010	0.79 ± 0.15	105 ± 12
O339	6	2.5	0.047 ± 0.009	0.38 ± 0.07	142 ± 10
O346	7	30	0.038 ± 0.007	0.17 ± 0.04	191 ± 34
O347	6	50	0.037 ± 0.008	0.16 ± 0.04	193 ± 32

at high count rates (>100 CPM). The apparent distribution volume is defined as $V = D/(\alpha_1 + \alpha_2)$, where D is the dose of labeled insulin. The clearance is calculated as $V\beta_1\beta_2(\alpha_1 + \alpha_2)/(\alpha_1\beta_2 + \alpha_2\beta_1)$, and the terminal half-life is given as $(\ln 2)/\text{minimum}(\beta_1, \beta_2)$.

RESULTS

Size-Exclusion Chromatography

The references for monomeric (X2) and hexameric insulin (Co(III)hexamer) as well as albumin (HSA) and albumin dimer (HSA dimer) are shown in Fig. 1A. Figure 1B shows the elution profiles of the insulin analogs in tris-buffered isotonic saline solution with 2 mM phenol. All the analogs except the monomeric O437 eluted with profiles similar to the reference Co(III)insulin hexamer, but area in the hexameric region of O381 (64% at 75 min.) indicated reduced hexameric stability with some dissociation. Analog O437 had a similar elution profile to the monomeric X2 reference. Figure 1C shows the elution profiles obtained after exclusion of phenol from the eluent, as is expected to occur in the injected subcutaneous depot of the pharmaceutical formulation. Here, insulin detemir eluted with a profile between the albumin and Co(III)insulin hexamer references, indicating an increased complex size following solute exchange. As this effect is dependent on the presence of 2 zinc per detemir hexamer stabilizing the hexamer moiety, the increase in size can be interpreted as a hexamer-dihexamer equilibrium. Furthermore, the crystal structure of insulin detemir displayed the fatty acids bound between the hexamer poles making specific interactions with the side chain of residue Phe^{B1} (32). This side chain has been deleted in analog O368, which still appeared as a hexamer at the same conditions. The unstable hexameric analog O381 (60% area at 75 min.) again had partial dissociation, and O437 again eluted as a monomer. Figure 1D shows profiles obtained by addition of 1% (150 μM) albumin to the eluent, to simulate the situation at the boundary (mixing zone) between the interstitial fluid and the injected depot. Here, labeled zinc added to the eluent eluted with a profile similar to albumin, indicating albumin binding of the zinc. However, zinc tracer added to the injected insulin detemir solution eluted *before* the albumin reference, indicating that the zinc was bound in a complex of greater molecular size than albumin. As zinc can bind to insulin detemir hexamers (which elute after albumin) as well as albumin, these observations indicate that insulin detemir hexamers are albumin-bound.

The insulin detemir tracer added to the eluent, in the nanomolar range, eluted just before albumin, indicating albumin-bound detemir monomers. The insulin detemir tracer included in the pharmaceutical formulation, in self-associated concentration, eluted before the zinc and also before the albumin dimer indicating that the predominant association form of insulin detemir in this *in vitro* model was a complex containing insulin detemir dimer and two albumin molecules. Consequently insulin detemir can only be albumin-bound as hexamer in the beginning of the size sorting proces of the *in vitro* model.

Disappearance of Subcutaneously Injected Insulin Analogs

The estimated $T_{75\%}$ and $T_{50\%}$ values for the disappearance of radioactivity from the injection depot are shown in Table I for the various insulin detemir and reference analog formulations. Additional reference data are provided for albumin, the stable, nondissociating hexameric Co(III)-insulin and the monomeric insulin analog X2.

The disappearance rates of the acylated analogs with similar albumin affinity to detemir, but with reduced hexamer-hexamer association (O368), indicated a significant difference relative to insulin detemir ($0.05 < p < 0.10$), whereas unstable hexameric structure (0381) was intermediate between those of insulin detemir and the monomeric 0437. All the hexameric insulins are characterized by longer $T_{50\%}$ values than the monomeric insulins, implying that insulin self-association makes an important contribution to increased depot residence time. The shorter $T_{50\%}$ of O368 (which does not dihexamerize) vs. insulin detemir implies that dihexamerizing further protracts the absorption. However, the much longer $T_{50\%}$ times of all the acylated hexameric insulins vs. Co(III)insulin (Table I) implies that albumin binding also plays an important part in protraction of absorption.

$T_{50\%}$ for a pharmaceutical formulation of 0.6 mM insulin detemir was found to be 10.2 h. A preservative-free formulation did not result in changed disappearance rates. The $T_{50\%}$ value for a 0.3 mM, zinc-free, 1:1 detemir:albumin formulation in saline solution was 7.3 h. The significance of this zinc-free formulation is that insulin detemir would be primarily dimeric. Reducing the insulin detemir concentration further to 0.003 mM, that is, below the dimerization threshold of 0.02 mM (33), in the presence of 0.3 mM albumin resulted in a $T_{50\%}$ of 3.8 h. These observations imply that insulin detemir self-association at the dimerization level has a high initial influence on delayed absorption. The monomeric analog O437 had a $T_{50\%}$ of 2.0 h in a pharmaceutical formulation, and of 3.7 h in a zinc- and preservative-free preformed 1:1

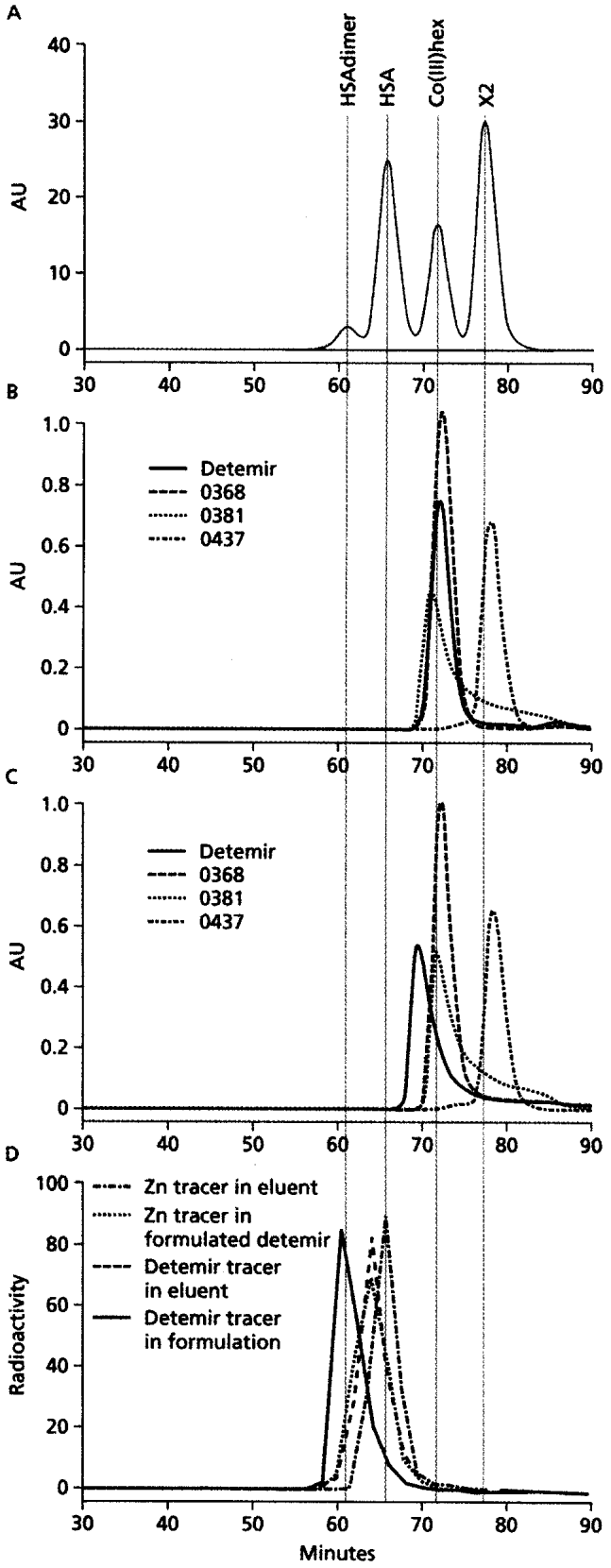

albumin complex. This suggests a major proportion of O437 is absorbed from the depot before binding to albumin. Thus, self-association appears necessary to delay absorption long enough for albumin binding to occur.

Fig. 1. Size-exclusion chromatography elution profiles in tris-buffered isotonic saline at 37°C of test compounds and references. (A) Reference molecules. (B) Tetradecanoic acylated insulin analogs in the presence of 2 mM phenol in the eluent. (C) Tetradecanoic acylated insulin analogs without phenol in the eluent. (D) Labeled zinc and detemir. Eluent without phenol, but containing 1% human serum albumin. Radioactivity was measured in the collected fractions.

Plasma Profiles of Acylated Insulin Analogs

The nonlinear regression analyses produced reliable individual parameter estimates in all cases. Figure 2 shows the close agreement between the observed mean data for insulin detemir and the fitted model. Similar close agreement was seen with the other acylated analogs. The inserted graph in Fig. 2 shows the data from which the distribution volume was determined in a separate experiment with 6 pigs given intravenous doses of D = 0.36 nmol/kg unlabeled detemir. The value of the fitted curve at time 0 min $C(0) = \alpha_1 + \alpha_2$ divided into D gives the distribution volume V = 0.052 L/kg. Because the dose of the various labeled acylated insulin analogs was the same, the distribution volumes were calculated as V multiplied by the ratio between the estimated count rates at time 0 for insulin detemir and for the other analogs. The mean volume of distribution, clearance rate and terminal long half-life for the acylated analogs are listed in Table II. The higher their affinity for PSA, the lower is the apparent volume of distribution and the lower the clearance rate. This finding suggests that the delay in insulin detemir reaching interstitial fluid from the blood (26,28) is probably attributable to serum albumin binding; 98–99% of insulin detemir is albumin-bound in the circulation (21,22). The terminal half-life of detemir in pigs is comparable to the value reported for dogs (26) and

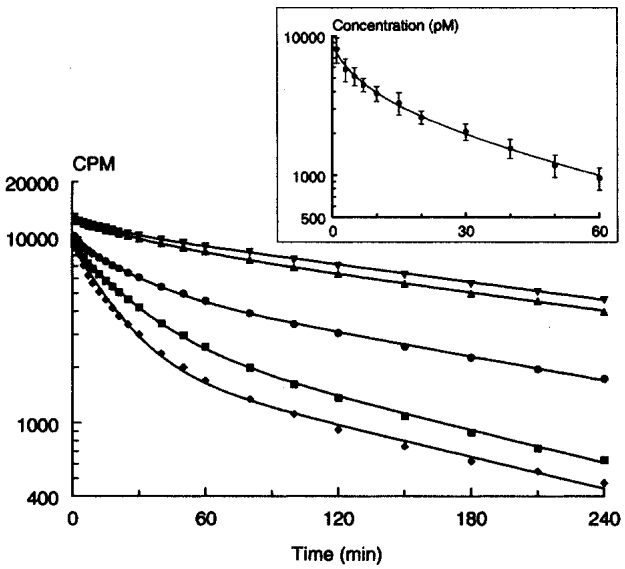

Fig. 2. Mean count rates of labeled acylated insulin analogs and fitted curves according to two-compartment model: (■) detemir, (●) O339, (♦) O344, (▲) O346, (▼) O347. The inserted graph shows the mean concentrations of unlabeled detemir (intravenous injection of 0.36 nmol/kg, 6 pigs) and the fitted curve. The estimated concentration at time 0 is used for calculation of the volume of distribution as described in the text.

much shorter than $T_{50\%}$ for the absorption from the subcutaneous depot (Table I).

DISCUSSION

Taken together, the data described in this report suggest a mechanism of protraction for insulin detemir that primarily involves hexamer association and subsequent albumin binding in the depot, followed by plasma albumin binding. It is anticipated that injection of the formulated insulin preparation initially will displace the interstitial fluid with minor mixing to surround the capillaries. Here, small molecules in the pharmaceutical formulation (phenol, cresol, and polyol) are lost from the solvent by diffusion through endothelial membranes. Simultaneously, sodium chloride will move into the depot to equilibrate serum ion strength. Under these conditions, data from SEC suggest that the association of insulin detemir increases from the hexameric state in the injected solution to a hexamer-dihexamer equilibrium. It is believed that dihexamers form by interaction between the fatty acid side chains; the 3-dimensional structure of the insulin detemir hexamer is such that three fatty acid chains are available for interaction at each pole of the hexamer complex (32). At the interface of the injected depot and the displaced interstitial fluid, preservative-depleted insulin detemir will come into contact with interstitial albumin. SEC showed that the addition of albumin to the eluent resulted in detemir-albumin binding. In the same system, the zinc tracer eluted before (at a larger molecular size) albumin, indicating that a part of insulin detemir is bound to albumin as hexamers, the zinc binding species.

In the porcine model of subcutaneous disappearance, $T_{50\%}$, was found to be 10.2 h for detemir. Acylated insulin analogs with similar albumin binding affinities to detemir, but unable to dihexamerize, having more unstable hexameric association, or existing only as monomers showed $T_{50\%}$ values of 8.8, 6.9, and 2.0 h, respectively, in the presence of zinc and phenol. These data suggest that the self-association state of these acylated insulins influences their absorption rate, with those insulins that remain hexameric being more slowly absorbed than those that dissociate. The apparent ability of insulin detemir to form dihexamers may explain its even greater retardation than the hexameric O368. However, all the acylated hexamers had much longer depot residence times than the stably hexameric Co(III) insulin, implying that albumin binding must contribute to the long residence time of insulin detemir. The comparison of $T_{50\%}$ for the monomeric O437 and its 1:1 albumin complex suggests that only a minor amount of this acylated insulin bound to albumin before absorption. The disappearance $T_{50\%}$ value of the preformed zinc-free insulin detemir-albumin formulation (in a 1:1 ratio, each at 0.3 mM) was 7.3 h, whereas dilution of detemir below its dimerization concentration threshold decreased $T_{50\%}$ to 3.8 h (i.e., equivalent to the monomeric O437–albumin complex). This observation suggests that at the 0.3 mM concentration, detemir forms a complex whereby dimers bind to two albumin molecules.

The SEC and subcutaneous absorption data collectively suggest, therefore, that insulins with more stable self-association states are more slowly absorbed than those that dissociate and that this may initially relate to physical constraints (i.e., their relatively impaired ability to penetrate capillary walls as well as to albumin binding of the associated forms). The greater retention in the depot may also increase the likelihood of albumin binding taking place, and albumin binding may subsequently act to "compensate" for dissociation of insulin detemir. This would explain the discrepancy between the $T_{50\%}$ values of the acylated analogs and Co(III) insulin. Thus, detemir's particularly long depot residence time is here regarded as due initially to the formation of dihexamers, with subsequent albumin binding.

Once insulin detemir is absorbed into the bloodstream, rapid and extreme dilution from the μM to pM range will cause immediate dissociation into monomers. Here, the albumin pool is vast and our data from porcine plasma profiling suggest that plasma albumin binding retards the distribution and elimination of insulins proportionally with albumin affinity. Sequestration by plasma albumin results in a retarded trans-epithelial transport (28). It is known that 98–99% of circulating insulin detemir is albumin bound (21,22), and previous kinetic studies in dogs have indicated that trans-epithelial transport of insulin detemir from blood into interstitium is indeed slow relative to human insulin (26–28). The $T_{50\%}$ for the absorption is, however, approximately six times higher than the long half-life of appearance and disappearance in interstitium. Thus, some protraction of distribution due to retention by plasma albumin follows the dominating protraction of absorption due to self-association and albumin binding. Once in the interstitial fluid, further albumin binding takes place. Due to the much higher affinity of insulin detemir for the insulin receptor compared to its affinity for albumin, and the vast number of available receptors, any further delay or protraction in the interstitial compartment is trivial (28). In early clinical studies intrasubject variation in fasting plasma glucose has been significantly lower in insulin detemir-treated patients compared to NPH treatment (14,37). Reduced pharmacokinetic and dynamic variability may have contributed to significant risk reduction for hypoglycemia in detemir treated patients, with this benefit being achieved without compromise in fasting plasma glucose or overall glycemic control (14,37).

In summary, the results of our experiments suggest that the subcutaneous absorption of insulin detemir is delayed and protracted initially through hexamer stability and dihexamerization and subsequently by albumin binding to the associated forms within the depot. The absorption rate is likely to remain fairly constant despite changes in the depot environment in the hours following injection. In the circulation, some further protraction is achieved by retention through albumin binding. The model proposed here is consistent with preliminary pharmacological and clinical observations in man, and describes a desirable profile for a basal insulin with increased predictability.

ACKNOWLEDGMENTS

We thank Ulla D. Larsen for provision of mono-[^{125}I]-iodo-Tyr^{A14}-insulin analogs and Lene G. Andersen, Pia S. Andersen, Lene V. Voss, Hanne Jensen-Holm, Birgitte Roed, Birgit D. Spon, and Yvonne B. Madsen for excellent technical assistance.

REFERENCES

1. S. O. Emdin, G. G. Dodson, J. M. Cutfield, and S. M. Cutfield. Role of zinc in insulin biosynthesis. Some possible zinc-insulin

interactions in the pancreatic B-cell. *Diabetologia* **19**:174–182 (1980).
2. S. Kang, J. Brange, A. Burch, A. Volund, and D. R. Owens. Subcutaneous insulin absorption explained by insulin's physicochemial properties. Evidence from absorption studies of soluble human insulin and insulin analogues in humans. *Diabetes Care* **14**:942–948 (1991).
3. P. Hildebrandt, P. Sejrsen, S. L. Nielsen, and K. Birch. and L. Sestoft Diffusion and polymerisation determine the insulin absorption from subcutaneous tissue in diabetic patients. *Scand. J. Clin. Lab. Invest.* **45**:685–690 (1985).
4. J. Brange, U. Ribel, J. F. Hansen, G. Dodson, M. T. Hansen, S. Havelund, S. G. Melberg, F. Norris, K. Norris, L. Snel, A. R. Sørensen, and H. O. Voigt. Monomeric insulins obtained by protein engineering and their medical implications. *Nature* **333**:679–682 (1988).
5. T. Lauritzen, O. K. Faber, and C. Binder. Variation in insulin absorption and blood glucose concentrations. *Diabetologia* **17**: 291–295 (1979).
6. P. Hildebrandt. Subcutaneous absorption of insulin in insulin-dependent diabetic patients. *Dan. Med. Bull.* **38**:337–346 (1991).
7. J. Brange, D. R. Owens, S. Kang, and A. Volund. Monomeric insulins and their experimental and clinical implications. *Diabetes Care* **13**:923–954 (1990).
8. J. Brange and A. Volund. Insulin analogs with improved pharmacokinetic profiles. *Adv. Drug Deliv. Rev.* **35**:307–335 (1999).
9. G. B. Bolli. Physiological insulin replacement in type 1 diabetes mellitus. *Exp. Clin. Endocrinol. Diabetes* **109**:S317–S332 (2001).
10. A. M. Gualandi-Signorini and G. Giorgi. Insulin formulations – a review. *Eur. Rev. Med. Pharmacol. Sci.* **5**(3):73–83 (2001).
11. P. Home. Insulin glargine: the first clinically useful extended-acting insulin in half a century? *Exp. Opin. Invest. Drugs* **8**:307–314 (1999).
12. G. B. Bolli and D. R. Owens. Insulin glargine. *Lancet* **356**:443–445 (2000).
13. D. R. Owens, B. Zinman, and G. B. Bolli. Insulins today and beyond. *Lancet* **358**:739–746 (2001).
14. K. Hermansen, S. Madsbad, H. Perrild, A. Kristensen, and M. Axelsen. Comparison of the soluble basal insulin analog insulin detemir with NPH insulin. A randomised open crossover trial in type 1 diabetic subjects on basal-bolus therapy. *Diabetes Care* **24**:296–301 (2001).
15. D. R. Owens, P. A. Coates, S. D. Luzio, J. P. Tinbergen, and R. Kurzhals. Pharmacokinetics of ^{125}I-labelled insulin glargine (HOE 901) in healthy men. Comparison with NPH insulin and the influence of different subcutaneous injection sites. *Diabetes Care* **23**:813–819 (2000).
16. J. Markussen, P. Hougaard, U. Ribel, A. R. Sørensen, and E. Sørensen. Soluble, prolonged-acting insulin derivatives, I: Degree of protraction and crystallizability of insulins substituted in positions A17, B8, B23, B27 and B30. *Protein Eng.* **1**:205–213 (1987).
17. J. Markussen, I. Diers, A. Engesgaard, M. T. Hansen, P. Hougaard, L. Langkjaer, K. Norris, U. Ribel, L. Snel, A. R. Sørensen, and H. O. Voigt. Soluble, prolonged-acting insulin derivatives. II. Degree of protraction and crystallizability of insulins substituted in positions A17, B8, B13, B27 and B30. *Protein Eng.* **1**:215–223 (1987).
18. G. B. Bolli, R. D. Di Marchi, G. D. Park, S. Pramming, and V. A. Koivisto. Insulin analogues and their potential in the management of diabetes mellitus. *Diabetologia* **42**(10):1151–1167 (1999).
19. L. Heinemann, R. Linkeschova, K. Rave, B. Hompesch, M. Sedlak, and T. Heise. Time-action profile of the long-acting insulin analogue insulin glargine (HOE901) in comparison with those of NPH insulin and placebo. *Diabetes Care* **23**:644–649 (2000).
20. M. Lepore, S. Pampanelli, C. Fanelli, F. Porcellati, L. Bartocci, A. Di Vincenzo, C. Cordoni, E. Costa, P. Brunetti, and G. B. Bolli. Pharmacokinetics and pharmacodynamics of subcutaneous injection of long-acting human insulin analog glargine, NPH insulin, and ultralente human insulin and continuous subcutaneous infusion of insulin lispro. *Diabetes* **29**:2142–2148 (2000).
21. P. Kurtzhals, S. Havelund, I. Jonassen, B. Kiehr, U. D. Larsen, U. Ribel, and J. Markussen. Albumin binding of insulin acylated with fatty acids: characterization of the ligand-protein interaction and correlation between binding affinity and timing of the insulin effects in vivo. *Biochem. J.* **312**:725–731 (1995).
22. J. Markussen, S. Havelund, P. Kurtzhals, A. S. Andersen, J. Halstrom, E. Hasselager, U. D. Larsen, U. Ribel, L. Schäffer, K. Vad, and I. Jonassen. Soluble fatty acid insulins bind to albumin and show protracted action in pigs. *Diabetologia* **39**:281–288 (1996).
23. P. Kurtzhals, S. Havelund, I. Jonassen, and J. Markussen. Effect of fatty acids and selected drugs on the albumin binding of a long-acting, acylated insulin analogue. *J. Pharm. Sci.* **86**:1365–1368 (1997).
24. L. Heinemann, K. Sinha, C. Weyer, M. Loftager, S. Hirschberger, and T. Heise. Time-action profile of the soluble, fatty acid acylated, long-acting insulin analogue NN304. *Diabet. Med.* **16**:332–338 (1999).
25. G. A. Brunner, G. Sendhofer, A. Wutte, M. Ellmerer, B. Sogaard, A. Siebenhofer, S. Hirschberger, G. J. Krejs, and T. R. Pieber. Pharmacokinetic and pharmacodynamic properties of long-acting insulin analogue NN304 in comparison to NPH insulin in humans. *Exp. Clin. Endocrinol. Diabetes* **108**:100–105 (2000).
26. M. Hamilton-Wessler, M. Ader, M. Dea, D. Moore, P. N. Jorgensen, J. Markussen, and R. N. Bergman. Mechanism of protracted metabolic effects of fatty acid acylated insulin, NN304, in dogs: retention of NN304 by albumin. *Diabetologia* **42**:1254–1263 (1999).
27. M. Hamilton-Wessler, M. Ader, M. K. Dea, D. Moore, M. Loftager, J. Markussen, and R. N. Bergman. Mode of transcapillary transport of insulin and insulin analog NN304 in dog hindlimb. Evidence for passive diffusion. *Diabetes* **51**:574–582 (2002).
28. M. K. Dea, M. Hamilton-Wessler, M. Ader, D. Moore, L. Schaffer, M. Loftager, A. Volund, and R. N. Bergman. Albumin binding of acylated insulin (NN304) does not deter action to stimulate glucose uptake. *Diabetes* **51**(3):762–769 (2002).
29. S. Havelund, J. B. Halstrøm, I. Jonassen, A. S. Andersen, and J. Markussen. Acylated insulin. European Patent EP 0 792 290 B1 (2002).
30. K. Drejer, V. Kruse, U. D. Larsen, P. Hougaard, S. Bjørn, and S. Gammeltoft. Receptor binding and tyrosine kinase activation by insulin analogues with extreme affinities studied in human hepatoma HepG2 cells. *Diabetes* **40**:1488–1495 (1991).
31. P. Kurtzhals and U. Ribel. A novel principle of protraction of potential use for basal insulin delivery. *Diabetes* **44**:1381–1385 (1995).
32. J. L. Whittingham, S. Havelund, and I Jonassen. Crystal structure of a prolonged-acting insulin with albumin-binding properties. *Biochemistry* **36**:2826–2831 (1997).
33. H. B. Olsen and N. C. Kaarsholm. Structural effects of protein lipidation as revealed by Lys^{B29}-myristoyl, des(B30) insulin. *Biochemistry* **39**:11893–11900 (2000).
34. H. B. Olsen, S. Ludvigsen, and N. C. Kaarsholm. The relationship between insulin bioactivity and structure in the NH_2-terminal A-chain helix. *J. Mol. Biol.* **284**:477–488 (1998).
35. M. Ellmerer, L. Schaupp, G. A. Brunner, G. Sendlhofer, A. Wuffe, P. Wach, and T. R. Pieber. Measurement of interstitial albumin in human skeletal muscle and adipose tissue by open-flow microperfusion. *Am. J. Physiol. Endocrinol. Metab.* **278**:E352–E356 (2000).
36. U. Ribel, K. Jørgensen, and U. Henriksen. The pig as a model for subcutaneous absorption in man. In: M. Serano-Rios and P. J. Lefebvre (eds.), *Diabetes. Proceeding of 12th Congress of the International Diabetes Federation, Madrid 1985*. Excerpta Medica, Amsterdam, 1986, pp. 891–896.
37. P. Vague, J.-L. Selam, S. Skeie, I. D. Leeuw, J. W. F. Elte, H. Haahr, A. Kristensen, and E. Draeger. Insulin detemir is associated with more predictable glycemic control and reduced risk of hypoglycemia than NPH insulin in patients with type 1 diabetes on a basal-bolus regimen with premeal insulin aspart. *Diabetes Care* **26**:590–596 (2003).
38. L. Heinemann, K. Sinha, C. Weyer, M. Loftager, S. Hirschberger, and T. Heise. Time-action profile of the soluble, fatty acid acylated, long-acting insulin analogue NN304. *Diabet. Med.* **16**:332–338 (1999).